UC Santa Barbara
UC Santa Barbara Previously Published Works

Title

Can Managed Aquifer Recharge Mitigate the Groundwater Overdraft in California's Central Valley?

Authors

Alam, Sarfaraz
Gebremichael, Mekonnen
Li, Ruopu
et al.

Alam Sarfaraz (Orcid ID: 0000-0002-9592-2782)

Li Ruopu (Orcid ID: 0000-0003-3500-0273)

Dozier Jeff (Orcid ID: 0000-0001-8542-431X)

Lettenmaier Dennis, P. (Orcid ID: 0000-0002-0914-0726)

Can Managed Aquifer Recharge mitigate the groundwater overdraft in California's Central Valley?

Sarfaraz Alam[1]*, Mekonnen Gebremichael[1], Ruopu Li[2], Jeff Dozier[3], and Dennis P Lettenmaier[4]

[1]Department of Civil and Environmental Engineering, University of California, Los Angeles, CA, USA. [2]School of Earth Systems and Sustainability, Southern Illinois University-Carbondale, Carbondale, IL, USA. [3]Bren School of Environmental Science & Management, University of California, Santa Barbara, CA, USA. [4]Department of Geography, University of California, Los Angeles, CA, USA

Corresponding author: Sarfaraz Alam (szalam@ucla.edu)

Key Points:

- The impact of managed aquifer recharge (MAR) on Central Valley's (CV) groundwater storage varies strongly from north to south.

- Absent movement of water from north to south, MAR can recover relatively little of the existing groundwater overdraft in the southern CV.

- Delivery of excess winter flows from the northern CV to the south would allow much of the existing groundwater overdraft to be mitigated.

Abstract

Groundwater plays a critical role in sustaining agriculture in California's Central Valley (CV). However, groundwater storage in the CV has been declining by around 3 km^3/year over the last several decades, with much larger declines during the 2007-2009 and 2012-2015 droughts. Managed Aquifer Recharge (MAR) can potentially mitigate existing overdraft by recharging excess streamflows (during flood periods) to the aquifers. However, the degree to which the existing CV groundwater overdraft might be mitigated by MAR is unknown. We applied a coupled surface water-groundwater simulation model to quantify the potential for groundwater overdraft recovery via MAR. To quantify the potential benefit of MAR, we used the coupled surface water-groundwater model to simulate water allocation scenarios where streamflow above the 90th or 80th percentiles was reallocated to aquifers, subject to constraints on the maximum depth of applied water (0.61m and 3.05m). Our results show that MAR could recover 9%-22% of the existing groundwater overdraft CV-wide based on a 56-year simulation (1960-2015). However, the impact of MAR varies strongly among regions. In the southern CV where groundwater depletion is most serious, the contribution of MAR to the overdraft recovery would be small, only 2.7%-3.2% in the Tulare basin and 3.2%-7.8% in the San Joaquin basin. However, transferring excess winter flow from the northern to the southern CV for MAR would increase the overdraft recovery to 30% in San Joaquin and 62% in Tulare. Our results also indicate that MAR has the potential to supplement summer low flows (52%-73%, CV-wide) and reduce flood peaks.

Plain Language Summary

California's Central Valley has experienced chronic groundwater depletion over the past half century. One mitigation strategy that has been widely discussed is to use excess winter floodwaters for groundwater banking (a.k.a., Managed Aquifer Recharge, or MAR). We conducted numerical experiments to assess groundwater storage changes in response to

selected MAR scenarios. Overall, MAR could recover most of the historical overdraft in the Sacramento and east of the Delta sub-basins, but much less in the most stressed San Joaquin and Tulare sub-basins where there is less excess water is available for MAR. Transferring excess flood waters from the Delta to the southern sub-basins would result in much greater aquifer recovery in those areas where historic overdrafts have been the greatest. Moreover, we find that MAR may have important ancillary benefits, including augmentation of low flows and flood risk reduction.

1 Introduction

Groundwater is an important freshwater source for more than 1.5 billion people globally (Alley et al., 2002). As the population grows and irrigated agriculture expands, reliance on groundwater continues to increase (Gorelick and Zheng, 2015; Rodell et al., 2009; Siebert et al., 2010). Overexploitation of groundwater due to increasing demand and climatic stresses (i.e. drought) in recent decades has had major, sometimes irreversible, impacts to many aquifers around the world (Taylor et al., 2013). For example, according to Wada et al. (2010), groundwater storage depletion rates have doubled over the past 50 years in arid and semi-arid regions of the world. Such large-scale depletion threatens sustainable agricultural development, as well as environmental and ecological health. Climate change is likely to further increase groundwater depletion rates by increasing irrigation water use and altering the timing and volume of streamflows (Alam et al., 2019; Hanson et al., 2012). Therefore, there is a critical need to identify vulnerable locations most affected by groundwater overdraft and measures to mitigate existing groundwater depletion.

The Central Valley (CV) of California, our study region, is one of the most agriculturally productive regions in the U.S. (Figure 1). It produces more than half of the fruits, nuts, and vegetables grown in the U.S. Almost half of the area in the CV is irrigated (~30,351 km^2),

using surface water, groundwater, or a combination of both. Surface water comes from upstream watersheds that surround the CV, the availability of which generally decreases from north to south following a north-south precipitation gradient. The regional imbalance in the surface water supply is mitigated somewhat by a complex surface water transfer network (Brown et al., 2009). Nonetheless, surface water alone is insufficient to meet water demands, and the deficit has been met by groundwater pumping, which now substantially exceeds recharge (Famiglietti et al., 2011; Li et al., 2018). Historically, groundwater has played a vital role in sustaining high agricultural productivity in the CV, especially during drought years.

Overexploitation of groundwater in the CV has resulted in progressive groundwater depletion. Long-term groundwater depletion rates have been estimated by several studies: about 3 km^3/year by Alam et al. (2019), 2.5 km^3/year by Hanak et al. (2017), 1.4-3 km^3/year by CDWR (2013), and 0.6-1.85 km^3/year by Faunt et al. (2009). GRACE satellite-based estimates show a depletion rate of around 20 km^3 (or about 2.2 km^3/year) over the period 2003-2011 (Famiglietti et al., 2011). Scanlon et al. (2012) estimated that the depletion rate in CV increased to about 8.9 km^3/year during the 2006-2009 drought, and Xiao et al. (2017) estimated a depletion rate of 11.2 ± 1.3 km^3/year during the 2012-2016 drought. Groundwater depletion in CV is expected to increase by about 2 km^3/year at the end of the century as the climate changes (Alam et al., 2019), absent implementation of mitigation measures. To minimize the impact of climate change and ensure groundwater sustainability, the California legislature passed the Sustainable Groundwater Management Act (SGMA) in 2014 to regulate the use of groundwater resources and to restore groundwater to an "acceptable level" by 2040 for critically over-drafted basins and 2042 for high and medium priority basins.

Several mitigation measures have been proposed to replenish the existing groundwater overdraft, including managing the demand and supply of water resources (Hanak et al.,

2019). A key mitigation measure that has been proposed by California's Department of Water Resources (CDWR) is Managed Aquifer Recharge (MAR), which would use excess flood flows (termed Flood-MAR) in the wet seasons to replenish aquifers via artificial recharge, primarily in the form of seasonal land flooding (CDWR, 2019; Sprenger et al., 2017). The benefits of MAR have been broadly recognized and have already been implemented in some parts of the CV (Dillon et al., 2019; Dillon et al., 2009; Scanlon et al., 2016). MAR has the potential to replenish aquifers, reduce land subsidence risk, increase drought resilience, and lower flood-related risks (Chinnasamy et al., 2018; Hashemi et al., 2015; Niswonger et al., 2017; Ronayne et al., 2017; Scanlon et al., 2016). MAR studies in California and elsewhere conducted at the local and farm levels (e.g., Bachand et al., 2014; Dahlke et al., 2018; Ghasemizade et al., 2019; Kourakos et al., 2019) demonstrate the potential of such practices to be scalable to the basin level. Strategies for implementing MAR on a more widespread basis are currently under investigation by CDWR (2018b, 2019). However, the benefits and limitations of MAR implementation at the scale of the entire CV are not well understood. There remain key questions, such as the extent to which MAR can replenish existing groundwater overdraft in the CV, and which regions have the greatest potential for MAR.

Here, we address the question of how much of the CV's groundwater overdraft can potentially be mitigated by MAR and how much the recovery may vary among regions and subregions of the CV. In addition, we examine the additional benefits of MAR for low flow augmentation and flood reduction.

2 Study Area

Figures 1a and 1b show the location of the CV region of California, which covers an area of about 53,600 km^2. As shown in Figure 1c, the CV generally has low relief and is surrounded by high-elevation watersheds (hereafter headwater watersheds) in the Sierra Nevada. Surface

water from these headwater watersheds flows into the CV through natural stream networks, and eventually enters the San Francisco Bay-Delta (hereafter Delta).

As shown in Figure 1c, CDWR divides the CV into five major hydrologic regions: Sacramento (SC, 15,900 km^2), Delta (DL, 2,900 km^2), East Delta (EZ, 3,660 km^2), San Joaquin (SJ, 10,020 km^2), and Tulare (TL, 21,200 km^2). The Sacramento, San Joaquin, and Tulare regions are located in the northern, central, and southern parts of CV respectively. The Delta and East-Delta hydrologic regions are located in the central CV and provide outlets to the Delta that drain excess surface water (remaining water that is not diverted for agricultural or municipal use) flowing through the rivers in the CV. As shown in Figure 1d, CDWR has further divided the region into 21 subregions for hydrologic studies. Here, we refer to each subregion using the IDs shown in Figure 1d (e.g., subregion 1 to be referred to as SR-1).

The long-term rainfall map (Figure 1d) shows that there is a strong precipitation gradient from the headwater watersheds to the valley floors, and from the northern part (which is mostly semi-humid) to the southern part (which is mostly semi-arid) of the region. The headwater watersheds in the north are generally rain-dominated and contribute most of the surface water flowing to the CV, while the southern headwater basins are snow-dominated. The north-south contrast in water demand and supply motivated the construction of the Central Valley Project (CVP) and State Water Project (SWP) aqueducts that transfer water from the Delta to the south via hundreds of miles of aqueducts. CVP, built in the 1970s and managed by the U.S. Bureau of Reclamation, is a multipurpose project consisting of dams, reservoirs, pumping plants, and aqueducts. The Friant Kern Canal (245 km length) and Delta Mendota Canal (188 km length) are the major CVP canals carrying water southward. SWP, currently operated by CDWR, is also a multipurpose project that was built about the same

time as the CVP. The California Aqueduct (length about 715 km) is the major SWP canal that
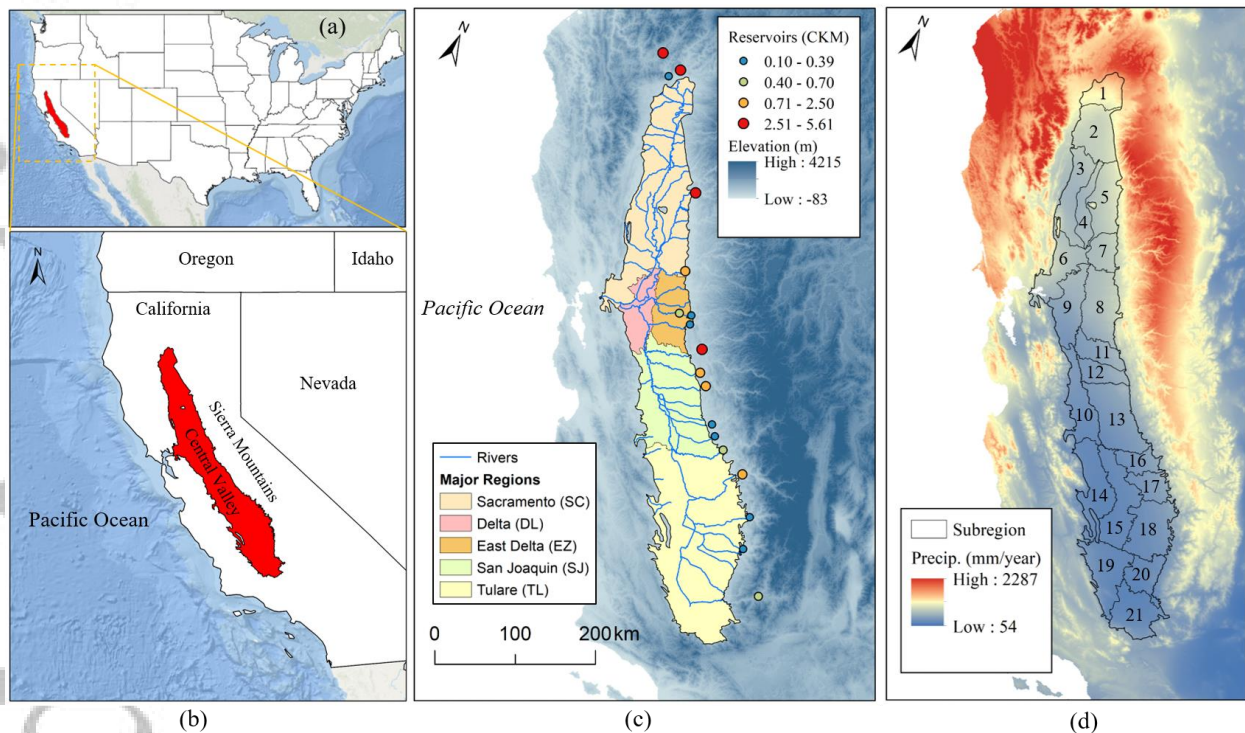
conveys water from north to south.

Figure 1. (a) Location of the CV in the U.S.; (b) CV location in California, (c) major

hydrologic regions (HR), major reservoirs, and river networks within the CV. Blue shade

represents elevation; and (c) 21 subregions (SR) of the CV, where the numbers represent the

ID of each subregion. Red to blue shade represents annual average precipitation (mm/year)

obtained from WorldClim global climate dataset (http://worldclim.org/).

There is also a temporal mismatch between rainfall and crop seasons: most of the

precipitation across the entire CV falls during the period of November to March, while

irrigation demand is mostly in the summer (July to September). This mismatch is mitigated

by some 18 major headwater reservoirs (locations shown as circles in Figure 1c), which store

winter flows for release during the summer (Alam et al., 2019). In addition to supplying

water during the low-flow season, the reservoirs provide additional benefits in the form of

flood protection and environmental services. The surface water that enters the CV is diverted at several locations to satisfy agricultural, municipal, and environmental needs taking into account water rights and legal requirements. Surface water flow in excess of the diverted water is discharged (exclusively in high-flow seasons) to the San Francisco Bay through the Delta.

3 Methodology

Our methodology involves numerical modeling experiments that use a coupled hydrologic model to simulate surface hydrology and groundwater dynamics. Figure 2 shows the five key steps of our modeling approach. The first step is to identify potential MAR sites based on soil properties and feasible locations for diverting streamflows to the recharge sites. The second step considers different water diversion rules (i.e., the maximum amount of water that can be diverted from the streams to the MAR sites). The third step is to conduct numerical modeling experiments using the coupled hydrologic model, CDWR's California Central Valley Groundwater-Surface Water Simulation Model (C2VSIM), and taking into consideration operational information such as suitable MAR sites, diversion locations, and diversion rules identified in previous steps. The fourth step is the analysis of model simulation results focusing on: (i) groundwater recovery, (ii) changes in the water balance, and (iii) low-flow augmentation, flood-risk reduction, and potential crop damage. In the following sections, we discuss each of these steps in further detail.
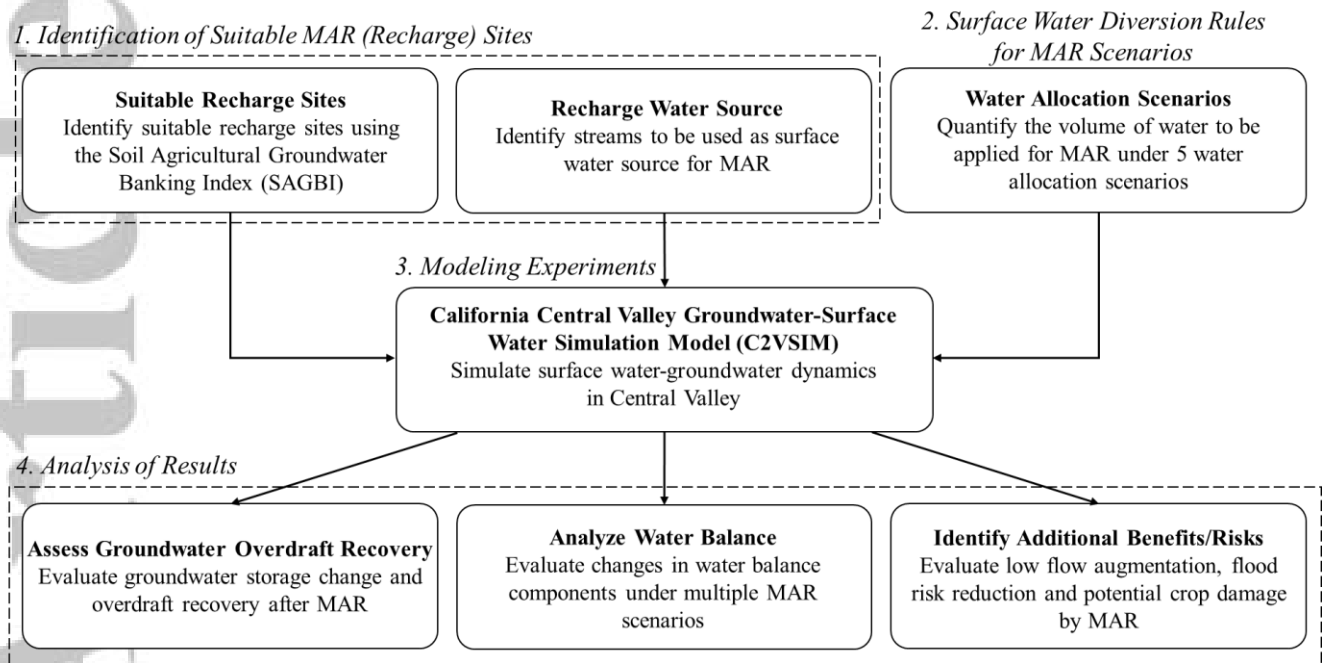
1. Identification of Suitable MAR (Recharge) Sites

Suitable Recharge Sites Identify suitable recharge sites using the Soil Agricultural Groundwater Banking Index (SAGBI)	**Recharge Water Source** Identify streams to be used as surface water source for MAR

2. Surface Water Diversion Rules for MAR Scenarios

Water Allocation Scenarios Quantify the volume of water to be applied for MAR under 5 water allocation scenarios

3. Modeling Experiments

California Central Valley Groundwater-Surface Water Simulation Model (C2VSIM) Simulate surface water-groundwater dynamics in Central Valley

4. Analysis of Results

Assess Groundwater Overdraft Recovery Evaluate groundwater storage change and overdraft recovery after MAR	**Analyze Water Balance** Evaluate changes in water balance components under multiple MAR scenarios	**Identify Additional Benefits/Risks** Evaluate low flow augmentation, flood risk reduction and potential crop damage by MAR

Figure 2. The flowchart used in our modeling experiment.

3.1 Model description

C2VSIM was developed by applying the Integrated Water Flow Model (IWFM) software (Dogrul et al., 2017) to the entire CV. We chose this model for a number of reasons. First, it was developed, calibrated, and validated for the CV, taking into account the main hydrological processes in the region. Second, the use of C2VSIM facilitates the communication and transfer of results to CDWR. CDWR has made Flood-MAR a priority, and is soliciting inputs from the community (an example is the October 2019 Flood-MAR Public Forum organized by).

C2VSIM is an integrated surface water and groundwater model that is capable of simulating hydrologic processes including surface runoff, streamflow, land surface, root zone and vadose zone processes, and saturated groundwater flow (Brush et al., 2013). Its core is a finite element solver, which has been implemented at both coarse-grid (C2VSIM-CG) and fine-grid (C2VSIM-FG) resolutions. We used a beta version of C2VSIM-FG (C2VSim-FG

beta2) that has been developed using IWFM version 2015 (hereafter, we refer to this version of C2VSIM-FG as C2VSIM). Originally calibrated by Brush et al. (2013), C2VSIM has been applied in multiple previous studies in the region (e.g., Alam et al., 2019; Dogrul et al., 2016; Ghasemizade et al., 2019; Kourakos et al., 2019).

C2VSIM dynamically calculates agricultural and urban water demands, links these to groundwater pumping and surface water diversions, and adjusts water deliveries based on demands. C2VSIM requires user-inputs for precipitation, evapotranspiration, irrigation method, crop distribution, population, boundary inflow, and surface water delivery. The model calculates the runoff, return flow, infiltration, vertical movement of soil moisture in the root zone, and aquifer recharge. The amount of crop water demand unmet by surface water and root zone soil moisture is dynamically supplemented by groundwater pumping. Crop water demand is calculated based on crop evapotranspiration rates, irrigation efficiency, stream diversion, precipitation, and crop distribution. Surface water delivery is user-defined in C2VSIM, suggesting that the applied water for MAR is an input to the model. However, the model has the capability of adjusting the actual delivery based on water availability in the stream. For example, if the allocated surface water delivery (as input) is higher than the available streamflow in a month, the model adjusts the volume of water that is available for MAR. The unsaturated zone in C2VSIM is divided into the root zone and the deep unsaturated zone where the flow in the root zone is computed dynamically using a tipping bucket model's one-dimensional unsaturated flow equation. A portion of the water applied for irrigation can flow through the vadose zone and reach the saturated zone through infiltration and deep percolation. The model also allows the application of MAR water directly to the saturated zone as deep percolation, which we follow in a manner similar to other recent studies (Ghasemizade et al., 2019; Kourakos et al., 2019). This allows the model

to be computationally efficient and thereby suitable for multi-decadal analysis of the impacts of MAR (Ghasemizade et al. 2019).

C2VSIM simulates all the major infrastructure that substantially affects the movement of water within the CV. In C2VSIM, surface water deliveries are specified at 414 locations, which include diversions for agriculture, urban, MAR, and regional export/import via natural streams and aqueduct/canals. Diversions from major infrastructure include Delta export to both CVP and SWP, the Delta-Mendota Canal to different water districts, DMC to Mendota pool, California Aqueduct diversion (e.g. Kern county via Cross Valley Canal or CVC), CVC diversions, and Friant-Kern canal diversion (to Kings, Tule, Kaweah and Kern Rivers), among many others. In addition, the model also considers existing MAR projects including the California Aqueduct diversion to the Kern water bank and Arvin-Edison water storage district, Kings River diversion (to Fresno, Alta Irrigation District), and many others (see Brush et al. (2013) for detail). Among the existing recharge projects, the Kern water bank and Arvin-Edison are relatively large (areas of 81 km^2 and 526 km^2 respectively) with maximum annual recharge capacities of 0.56 and 0.19 km^3/year respectively, and cumulative storage volume ranges between 1 km^3 to 2 km^3 (Christian-Smith, 2013; Scanlon et al., 2012).

Figure 3 shows the major processes represented by C2VSIM. C2VSIM uses four vertical layers in the subsurface. The top layer represents the unconfined aquifer and the bottom two layers represent confined aquifers. The confined and unconfined aquifers are separated by a thin layer of Corcoran clay in parts of the modeling domain. Horizontally, the region is divided into finite element computational polygons, which have irregular shapes. Each corner of a finite element is called a groundwater node. C2VSIM uses the Galerkin finite element method to solve the governing equation at each groundwater node. Stream connectivity in C2VSIM is defined by a series of inflow and outflow nodes, which represent the locations

where the water is received from surface runoff, return flow, and other nodes, and where the water is diverted for irrigation and other downstream nodes. Stream-aquifer interactions depend on the head gradient between the stream stage and groundwater head, and streambed conductance.

The model operates at a monthly time step. We used the baseline period of 1960-2015 (water years). Therefore, our analyses are derived from 56 years of historical data (inputs) and corresponding monthly simulations.
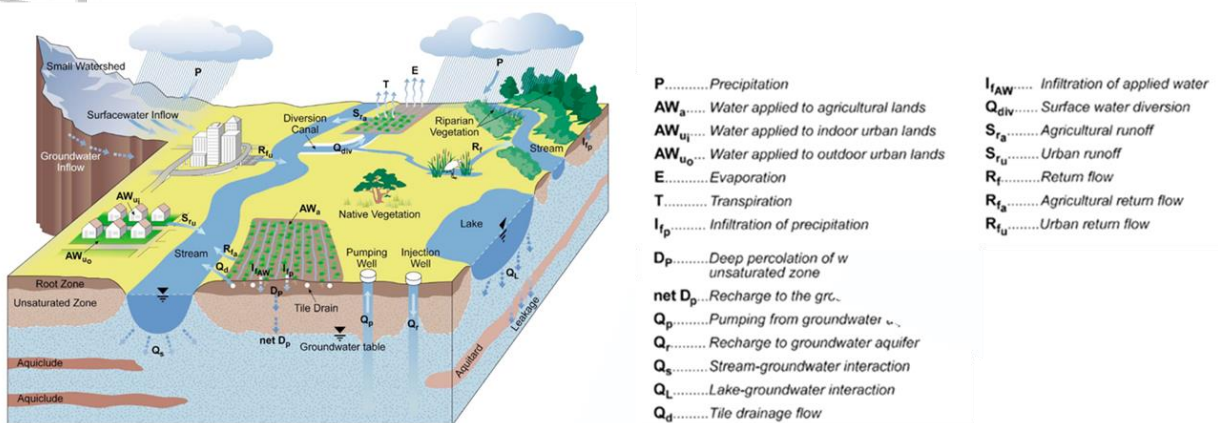

Figure 3. Major hydrologic processes modeled by the C2VSIM (IWFM manual)

3.2 Identification of suitable MAR (recharge) sites

We identified suitable recharge sites within each subregion using a two-step process. First, we identified potential sites suitable for recharge based on soil properties - this step classified the land into MAR-suitable and MAR-unsuitable areas. Then, we identified diversion locations on the streams within each of the 21 CDWR subregions (subregions without any stream were considered MAR-unsuitable regardless of suitability based on soil properties). The physical and geological characteristics of a recharge site determine the efficiency of

groundwater overdraft recovery by MAR (Ghasemizade et al., 2019). Recharge sites that consist of relatively coarse-grained soils (e.g. sand and gravel) have higher recharge rates compared to sites with fine-grained soils (e.g., clay). However, the selection of suitable recharge sites must be based on physical and geologic characteristics of the entire soil column, as the geologic formation of aquifers is heterogeneous both spatially and vertically (Fogg et al., 1986; Maples et al., 2019).
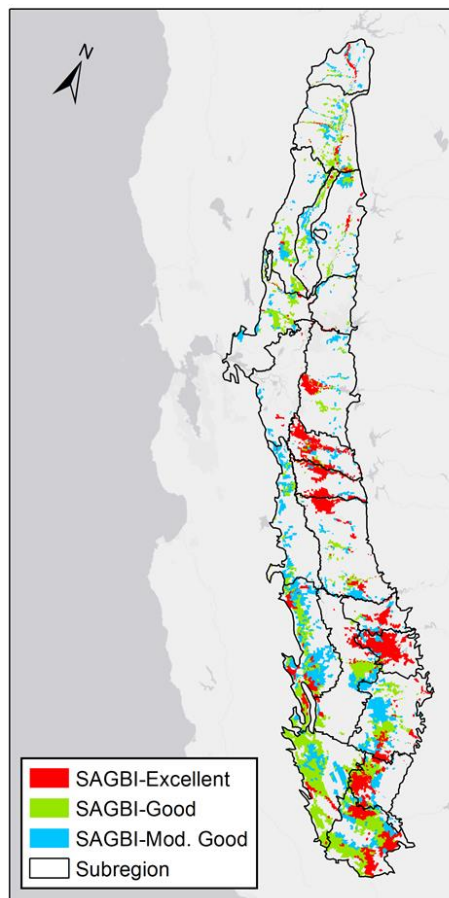

Figure 4. SAGBI classified excellent, good, and moderately good recharge sites in CV.

Table 1. Mar recharge site areas and water diversions by regions (in km^3/yr) for MAR under different scenarios. Here, SC, EZ, SJ, TL and CV represent Sacramento (SC), East-Delta (EZ), San

Joaquin (SJ), Tulare (TL) and Central Valley (CV) respectively. Figure 4 shows the spatial distribution of recharge sites.

Regions	SC	EZ	SJ	TL	CV
MAR recharge site areas (km^2)					
SAGBI-Excellent	317	770	2166	4844	8097
SAGBI-Good	1720	106	377	5209	7412
SAGBI-Moderately Good	1262	145	1060	3553	6020
Total area	3298	1021	3602	13607	21529
Water allocation in MAR scenarios (km^3/yr)					
R90_2ft	0.85	0.16	0.18	0.20	1.40
R80_2ft	1.44	0.26	0.32	0.30	2.32
R90_10ft	1.85	0.38	0.22	0.21	2.65
R80_10ft	3.17	0.61	0.42	0.30	4.50

We used the recharge-potential classification recommended by the Soil Agricultural Banking Index (SAGBI) that takes soil properties into account (O'Geen et al., 2015). The SAGBI classifies lands within the CV into six groups according to their suitability for MAR: excellent, good, moderately good, moderately poor, poor, and very poor. The SAGBI classification is based on the following factors: deep percolation, root zone residence time, chemical limitations, topographic limitations, and surface conditions. We used the unmodified version of the SAGBI (O'Geen et al., 2015) that considers the soil permeability derived from the USDA-NRCS Soil Survey Geographic Database (SSURGO) and ignores the effect of agricultural tillage. Since the focus of our study is to test the full potential (i.e. maximum) of MAR for groundwater overdraft recovery, we only considered locations with excellent, good, and moderately good soil suitability as potential recharge sites (see Figure 4). Because the SAGBI map identifies agricultural lands suitable for recharge, our MAR application is also known as agricultural managed aquifer recharge or Ag-MAR (hereafter, we will use MAR to refer to Ag-MAR). Table 1 shows the distribution of recharge sites we identified using SAGBI in major regions of the CV. The total recharge site area is highest in the TL region (roughly 4 times the recharge area of SC or SJ). Based on SAGBI, we found that there are more recharge sites with excellent suitability than there are good and moderately good recharge areas. Kourakos et al. (2019) studied the effect of MAR in SR-3

using some of the SAGBI recharge areas which range between 42 and 154 km^2, whereas the potential recharge area we use in the entire SR-3 is 704 km^2. Ghasemizade et al. (2019) conducted numerical experiments with MAR scenarios in SR-18 with a recharge area ranging between 313 and 1023 km^2, which is roughly comparable with 1660 km^2 of suitable recharge areas we identified in SR-18. Although the SAGBI classification provides the best available information on the soil's MAR potential, we acknowledge that there are uncertainties associated with the representation of subsurface geologic structures that might not be well captured by SAGBI (Maples et al., 2019).
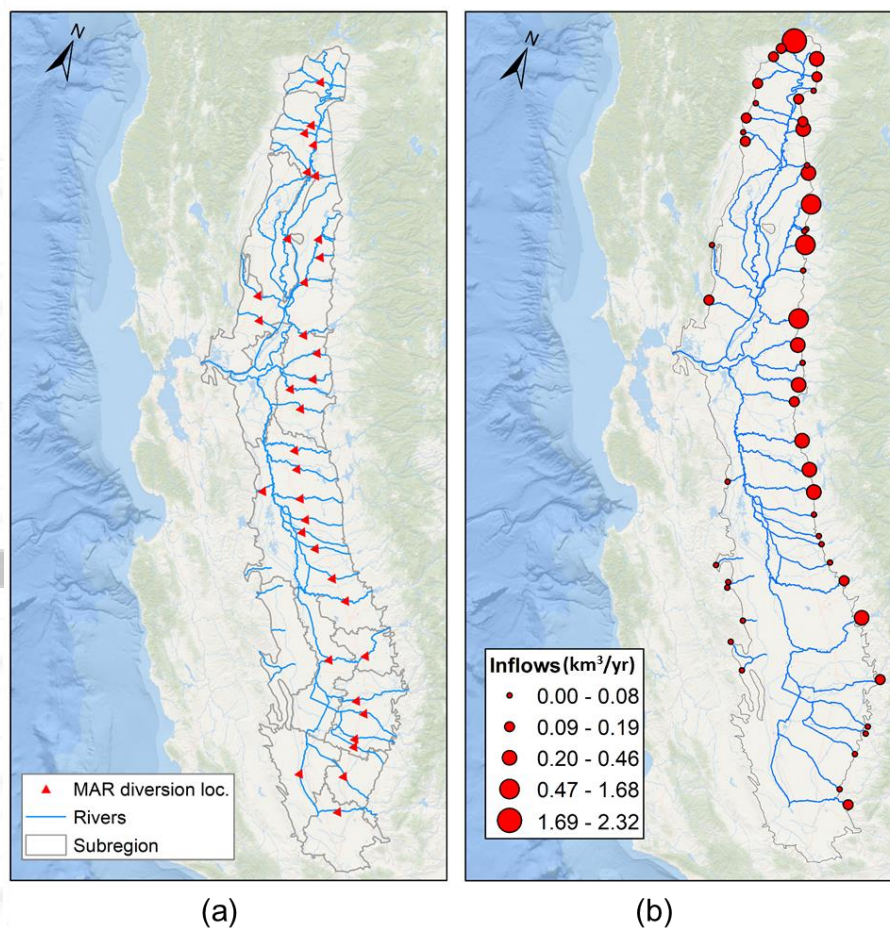
Figure 5. (a) Surface water diversion locations for MAR. (b) November-March headwater watershed inflow in km^3/year for the period 1960-2015.

Given the purpose of our study, we assumed that all the recharge sites within a given subregion would be uniformly recharged, provided that there is at least one stream crossing the region (more discussion below). However, in reality, the depth of water that can be applied to a recharge site may be limited by additional factors, such as the height of berms or the depth of recharge basins, conveyance structure capacity from hydraulic engineering perspectives, and crop sensitivity to stagnant water (for agricultural lands).

In the CV, the surface water originating from the headwater watersheds flows through interconnected rivers and enters the immediate downstream subregion, where it serves as a potential source of recharge water. We identified locations on the rivers where recharge water could be diverted to the MAR sites. Each subregion has either one, multiple, or no rivers crossing it (see Table S1 of Supplementary Material, which lists the diversion streams for each subregion). Assuming that all rivers crossing a given subregion could provide recharge water to that subregion, we identified only one diversion location on each river for each subregion (a subregion with no river is deemed unsuitable for MAR). For our modeling experiments, we identified exact diversion locations on the rivers for each subregion based on a simplified rule that the locations should have the minimum distance between a river and the center of recharge sites (diversion locations shown in Figure 5a; detailed selection criteria described in Text S1 of the Supplementary Information).

3.3 Surface water diversion rules for MAR scenarios

Surface water availability in the CV is highest during the winter (November through March) because most of the CV's annual precipitation occurs during this season. Figure 5b shows the annual average streamflow entering the CV from the headwater watersheds during the winter. The figure shows that the streamflow volumes are higher in the northern headwater watersheds compared to southern headwater watersheds. Once this streamflow enters the CV,

the water flows through connected rivers shown in Figure 5b, where it is diverted for agricultural and municipal purposes with the remaining water finally draining to the Delta. During 1960-2015, the average volume of winter Delta outflow was about 18 km^3/year. Delta outflow (on average) increases from December to January, and then remains stable up to March. There must be a minimum flow into the Delta to meet environmental and legal requirements. Flows above this requirement after meeting all the needs are referred to as "excess flow" (see Figure S1 of Supplementary Material for Delta outflow variability).

Surface water diversion rules for MAR depend on two factors: (1) streamflow requirements to meet environmental and legal restrictions in the streams and the Delta, and (2) allowable depth of water at the recharge sites that can realistically be retained for recharge and would not affect the production of winter crops if the land is used for agricultural purposes. Here, we made assumptions and used theoretical values to incorporate these two factors as discussed below.

With respect to the first factor, no fixed rule is available in most streams flowing to the CV as to how much excess flow might be diverted for MAR without causing environmental conflicts. However, there is a general consensus that streamflow above the 90th percentile threshold (during the period November to March) could be considered for MAR allocation (Baker et al., 2004; Kocis and Dahlke, 2017; Olden and Poff, 2003; USGS, 2016). Therefore, we calculated the 90th percentile of winter flow at each diversion location (shown in Figure 5a), and considered winter flows that exceeded the 90th percentile threshold for MAR application in corresponding subregions (referred to as the R90 scenario). We tested a less restrictive threshold, the 80th percentile (R80 scenario), as well. At a field scale, the volume of water that can actually be applied depends on the existence of a conveyance system and its capacity to carry water to the recharge sites. We assume the allocated water can be delivered

to the MAR sites even if there is no existing conveyance system for delivery, i.e., a lack of conveyance system is not a constraint. As noted in section 4.8, in this respect we provide a maximum or bounding estimate of the potential of MAR.

MAR can negatively affect winter crops in the recharge sites if the sites are agricultural land and water is left stagnant for long periods. However, most of the recharge sites we identified are located in agricultural lands. On agricultural lands, water is retained by building a berm (elevated border using soil) that generally has a height of 0.153 m or 6 inches (Flores-López, 2019). If water is applied each day, assuming all water is recharged, the total depth it can hold in a month is 2.29 m or 15 ft (6-inch × 30-days). To be conservative but also realistic, assuming recharge over 2/3 of the month, such a recharge site can allow up to 3.05 m (or 10ft) recharge in a month. Here, we adopted a maximum depth of 3.05 m (10 ft) as well as a more restrictive option of 0.61 m (2 ft) per month in our scenario experiments. In both scenarios, we applied water uniformly to all recharge sites.

To implement both scenarios, we followed a two-step process to determine the actual volume of water to be applied. In the first step, we quantified the volume of water available from a stream above the threshold (90th or 80th percentile). Second, we calculated the maximum volume of water allowed to be delivered to the recharge site in a given scenario, which is the product of the recharge area and maximum allowable depth (0.61 or 3.05 m). If the water available is less than the maximum allowable delivery, all water is delivered; otherwise, the application volume is equal to the maximum allowable delivery.

In summary, we considered four diversion rules:
- 90th percentile threshold with 0.61 m (or 2-ft) application depth (R90_2ft)
- 90th percentile threshold with 3.05 m (or 10-ft) application depth (R90_10ft)
- 80th percentile threshold with 0.61 m (or 2-ft) application depth (R80_2ft)

- 80th percentile threshold with 3.05 m (or 10-ft) application depth (R80_10ft)

The availability of surface water for recharge has been identified as one of the most critical factors to the success of MAR (Perrone and Merri Rohde, 2016). Earlier studies have quantified the volume of surface available for MAR using both monthly and daily streamflows. CDWR (2018a) estimated regionwide water available for recharge using a hydrological model (WEAP) in combination with gage measurements. The study used simulated monthly streamflow from WEAP, and estimated water available for recharge considering both unlimited and limited conveyance capacities (i.e. based on historical maximum diversion). On this basis, they found 0.82 and 0.27 km^3/year water available for recharge in SC and SJ_TL (SJ and TL together) respectively under limited conveyance capacity. CDWR (2018a) found 5 and 0.85 km^3/year water available for recharge in SC and SJ_TL respectively considering unlimited conveyance capacity. Kocis and Dahlke (2017) estimated the amount of water available for groundwater recharge using daily streamflows and found 2.0 and 1.2 km^3/year water available for recharge in SC and SJ_TL. Table 1 shows our estimate of annual average water diversions for MAR during 1960-2015 for each major region (MAR allocation for each subregion is presented in Table S2 of Supplementary Material). We calculated the water available for recharge based on simulated monthly streamflow from C2VSIM. The diversion volumes are higher in the north, due to higher excess water availability. In contrast, the diversion volumes in the south are less variable due to relatively low winter inflows. In our case, we used a monthly time step, as did CDWR (2018a). We found that water available for MAR in SC is 0.85 and 1.85 km^3/year under R90_2ft and R90_10ft scenarios respectively. For SJ_TL, our estimated water available for recharge are 0.38 and 0.43 km^3/year under R90_2ft and R90_10ft scenarios. Our estimate under the R90_2ft scenario is close to CDWR's estimate. In comparison with Kocis and Dahlke (2017), under the R90_10ft scenario, our estimate for SC is close (1.85 vs 2.0

km^3/year) but lower in SJ_TL (0.43 vs 1.2 km^3/year). The higher value by Kocis and Dahlke (2017) is most likely attributable to the daily time step they used. We acknowledge that the use of a monthly timestep can lead to a lower estimate of water available for recharge in some years due to not being able to capture peak flows from short term storms. However, we argue that the consideration of the 80th percentile threshold rather than the 90th percentile compensates for some of the time step-related differences.

In the above scenarios, streams (originating from headwater watersheds) crossing each sub-region are considered "source" water for MAR in each sub-region. Due to the spatial variability of rainfall (see Figure 1d), subregions in the northern part of CV are expected to receive more recharge water compared to subregions in the southern part. Similarly, northern regions contribute more excess Delta flow than the southern regions. We added one additional scenario in which the streamflows in the Delta that exceeded the 90th percentile threshold after the R90_2ft scenario being implemented were transferred to the southern subregions in the SJ and TL basins. We labeled this scenario as "R90_2ft_WT". In our case, we assumed that the existing infrastructure is capable of transferring water to the south (SJ and TL) for MAR.

In all the MAR scenarios described above, we limited our analysis to 56 years (1960-2015) a period that includes historical crop/land-use change and infrastructural developments. However, there are differences in infrastructural developments and crop/land use between the last decade and a few decades earlier. For example, SWP and CVP were fully developed by the mid-1980s, after which the Delta operation was different than before. Moreover, there have been changes in cropping patterns (mostly transition of row crops to tree crops) and some other land uses over the decades. To expand our analysis to potential future conditions, we conducted additional experiments with crop/land use and infrastructure development

representative of the recent past. To do so, we performed three additional simulations with land use and cropping patterns fixed at the year 2009 (here, we assume 2009 land use is representative of current conditions). These three simulations are (1) base_cf: base simulation with fixed cropping and land use pattern, (2) R90_2ft_cf: R90_2ft simulation with fixed cropping and land use pattern, (3) R90_10ft_cf: R90_10ft simulation with fixed cropping and land use pattern. We consider the post-1980 period (1980-2015) for the above scenarios, which is representative of current (expected) infrastructural development. The differences between in R90_2ft_cf (and R90_10ft_cf) and base_cf provide an insight into the expected groundwater changes if infrastructural development and water footprint stay the same for the recent and future periods.

4 Results and discussion

4.1. Surface water delivery under MAR

In section 3.3, we discussed the volume of water allocated for MAR in different regions of CV. The volume of water that is actually diverted depends on the water availability in the stream. Table 2 presents the regionwide distribution of actual volumes of MAR delivery simulated by C2VSIM. We found that the actual volume of water delivered is nearly the same as the allocation in all the regions. For example, water allocations for SC under the R90_2ft and R90_10ft scenarios are 0.85 and 1.85 km^3/year, whereas the actual delivery is 0.82 and 1.77 km^3/year respectively. We found that the actual delivery under the R90_2ft scenario for SC and SJ_TL were close to those reported by CDWR (2018a), i.e. SC (CDWR: 0.82 vs. ours: 0.82 km^3/year) and SJ_TL (CDWR: 0.27 vs. ours: 0.29 km^3/year). We also found that the actual volume of deliveries in TL did not increase as the depth of water application increased from 0.61 m (or 2 ft) to 3.05 m (or 10 ft). This is attributable to the fact that the

total recharge area is large enough to allocate all the water for either threshold depth (0.61 m or 3.05 m).

Table 2. Actual volume of water delivery (km^3/year) for MAR in all major regions.

Regions	R90_2ft	R80_2ft	R90_10ft	R80_10ft
SC	0.82	1.37	1.77	3.04
EZ	0.15	0.22	0.28	0.40
SC_EZ	0.97	1.59	2.05	3.44
SJ	0.18	0.32	0.22	0.42
TL	0.11	0.15	0.11	0.15
SJ_TL	0.29	0.47	0.32	0.57
CV	1.25	2.06	2.37	4.01

Note: SC_EZ: SC and EZ together, SJ_TL: SJ and TL together

4.2 Groundwater storage change

4.2.1 Baseline groundwater storage change during 1960-2015

First, we quantified the groundwater storage change between the end-years of the baseline period, 1960 and 2015, for each of the subregions (Figure. 6a). The change in groundwater storage varies within the region. In general, the southern region (almost half of the CV) has the most serious groundwater overdraft problem, while the northern region has exhibited little to no change in groundwater storage in recent decades. The groundwater overdraft in the southern CV is severe: the largest overdraft of 0.71 km^3/yr in SR-18 in the TL. The next largest overdrafts are between 0.41 km^3/yr and 0.40 km^3/yr in SR-10 (SJ basin) and SR 17 (TL basin) respectively. The north-south gradient in groundwater overdraft is due to increasing gaps in surface water supply and agricultural water demand. On average, CV groundwater storage has decreased by about 3.1 km^3/year during 1960-2015. We estimated that groundwater storage has been changing at a rate of 0.28, -1.01, and -2.28 km^3/year in the SC, SJ, and TL regions respectively from 1960-2015. The regionwide distribution of groundwater change was also estimated by Faunt et al. (2009), who used the CVHM model for CV groundwater depletion. They found that groundwater storage had changed at a rate of

0.04, -0.03, and -2 km^3/year in the SC, SJ, and TL respectively from 1962-2003. Hanak et al. (2018) estimated groundwater changes in SJ and TL from 1986-2015 and found that groundwater storage had changed at a rate of -0.2 and -2 km^3/year in SJ and TL respectively. Overall, our estimated groundwater storage depletion rate in CV is higher compared to Hanak et al. (2017) and Faunt et al. (2009). Regional comparison with other studies shows that our estimated groundwater storage change rate is similar for TL, higher in SC and lower in SJ.

4.2.2 Impact of MAR on groundwater storage change in subregions

We evaluated the groundwater storage changes for the R90 (R90_2ft and R90_10ft) and R80 (R80_2ft and R80_10ft) MAR scenarios. The spatial distribution of groundwater storage change for MAR scenarios have similar patterns as the base scenario. We found that the groundwater storage change under R90_2ft, R90_10ft, R80_2ft, and R80_10ft scenarios was -2.8 km^3/year, -2.6 km^3/year, -2.6 km^3/year and -2.4 km^3/year respectively during 1960-2015. We also calculated the percent change in groundwater storage by MAR for each subregion using Equation (1),

$$\text{GWC}(\%) = \frac{\sum_{i=1}^{N} \Delta GW_{i,MAR} - \sum_{i=1}^{N} \Delta GW_{i,base}}{abs(\sum_{i=1}^{N} \Delta GW_{base})} \times 100 \qquad (1)$$

where, GWC represents the groundwater storage change in percentage after MAR application compared to the base condition. The term GWC also represents groundwater overdraft recovery (%) when there is an overdraft in the base simulation. ΔGW_i represents groundwater change in a given month i compared to previous month. N is total number of months (N=672 months in our case) and *abs* represents the absolute value.
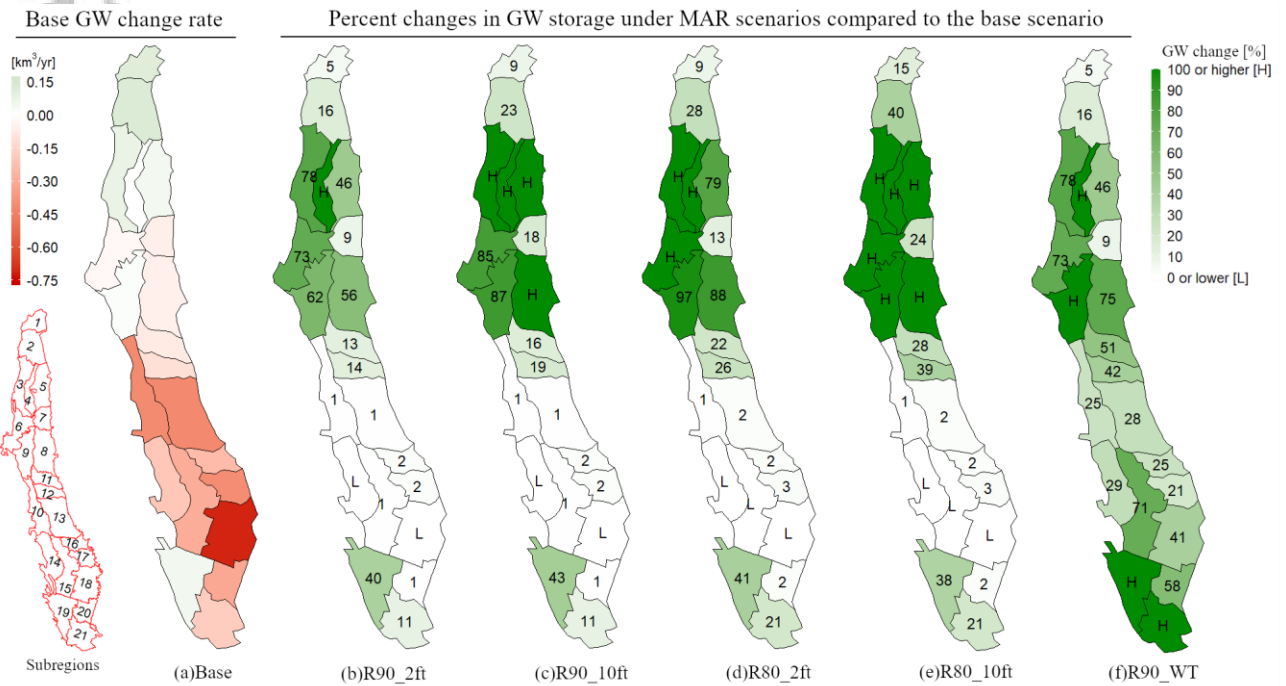
Figure 6. (a) Groundwater storage change rates (km³/year) in the base simulation (year 1960-2015), where the unit km³/year represents the annual average groundwater change in a subregion. (b-f) Groundwater storage changes (%) compared to base conditions for R90_2ft, R90_10ft, R80_2ft, R80_10ft, and R90_WT scenarios respectively. The inset map on the left corner shows the subregion IDs.

Figure 6b-e show GWC under R90_2ft, R90_10ft, R80_2ft, and R80_10ft scenarios. In SC_EZ, subregions 2 to 8 show higher GWC, which is due to a higher amount of water applied to areas with relatively small or no groundwater overdraft. Results from the base scenario show that only SR-6, SR-7, and SR-8 have an existing groundwater overdraft (Figure 6a) in SC_EZ. MAR would mitigate more than half of the existing groundwater overdraft in SR-6 (GWC 73%-100%) and SR-8 (GWC 56%-100%), and up to 25% in SR-7. The rate of groundwater storage change is low in SJ and TL subregions, except for SR-11 and SR-12 that show higher change. The low percentages for most of the SJ and TL subregions (Figure 6b-e) are due to low net groundwater recharge compared to a relatively high existing overdraft. In TL, only SR19 shows high (compared to the rest of the domain) GWC, which is

due to relatively low groundwater storage change in the base scenario compared to other subregions in TL.

4.2.3 Impact of MAR on groundwater storage change in major hydrologic regions

Figure 7a shows the percent change in groundwater storage in each of the major hydrologic regions (HRs) (see Figure S2 in Supplementary Material for the cumulative difference in groundwater storage between MAR and base scenarios). Groundwater storage change is calculated using Equation (1). We found MAR can recover 8.9% and 14.1% of the CV's total groundwater overdraft (we use the term overdraft when base scenario shows groundwater loss) under the R90_2ft and R80_2ft scenarios, respectively. The recoveries under R90_10ft and R80_10ft are 14% and 22.2%. Groundwater storage change is highest in SC_EZ, ranging from 27.5% to 57.3% under the R90 scenarios (R90_2ft and R90_10ft) and, 56% to 101% under R80 scenarios (R80_2ft and R80_10ft). The relatively high change in SC_EZ is attributable to the higher availability of excess surface flow. In SJ, the overdraft recoveries range from 3.2% to 7.8%. Recoveries are even lower in TL, where only 2.7% to 3.2% of the existing overdraft can be recovered by any scenario. Our findings indicate that the lack of floodwater (without water transfers from the Delta) is the key reason for low groundwater overdraft recovery (in SJ and TL), rather than the lack of recharge sites (assuming implementation of MAR at all selected locations). Low groundwater recovery in SJ and TL is due to low water availability combined with high existing overdrafts, which is also evident in other studies (e.g. Ghasemizade et al., 2019). It appears that SJ and TL will require measures in addition to MAR to mitigate the existing overdraft. These include, for example, moving from crisis-driven responses (e.g. groundwater overexploitation during drought) to the enactment of mitigation measures (e.g. conjunctive management, cropping pattern shift, irrigation efficiency) (Christian-Smith et al., 2015). Xiao et al. (2017) showed that a shift in

cropping pattern (predominantly row crops to tree crops) has contributed to enhanced groundwater depletion during the 2012-2015 drought. Alam et al. (2019) estimated an increase in groundwater depletion rate of 0.93 km^3/year for a 40% shift from row to tree crops. Further study is required to assess the combined effect of demand management along with MAR.

4.2.4 Groundwater storage change under water transfer scenario R90_2ft_WT

As described in section 3.3, we quantified the volume of water leaving the Delta above the 90th percentile (excess flow) after implementing the region-wide R90_2ft scenario, which is about 2.2 km^3/year (see Figure S3 of Supplementary Material for the cumulative difference in Delta outflow between MAR and base scenarios). We applied this water to the recharge sites of SJ and TL. The total volume of transferred water applied to SJ is on average 0.41 km^3/year and TL is 1.79 km^3/year under the R90_2ft_WT scenario. Figure 6f shows the spatial distribution of groundwater storage changes under the R90_2ft_WT scenario. We found that SR-15, 18, 19, and 21 show higher groundwater storage changes. Figure 7a compares the groundwater storage change percentage between water transfer scenario R90_2ft_WT and non-water transfer scenarios. We found that the R90_2ft_WT scenario significantly increases groundwater storage change (or overdraft recovery) in SJ and TL; specifically the groundwater overdraft recovery increased to 63%, 62% and 30% (under R90_2ft_WT scenario) from 9%, 3% and 3% (under R90_2ft scenario) in CV, TL, and SJ respectively.
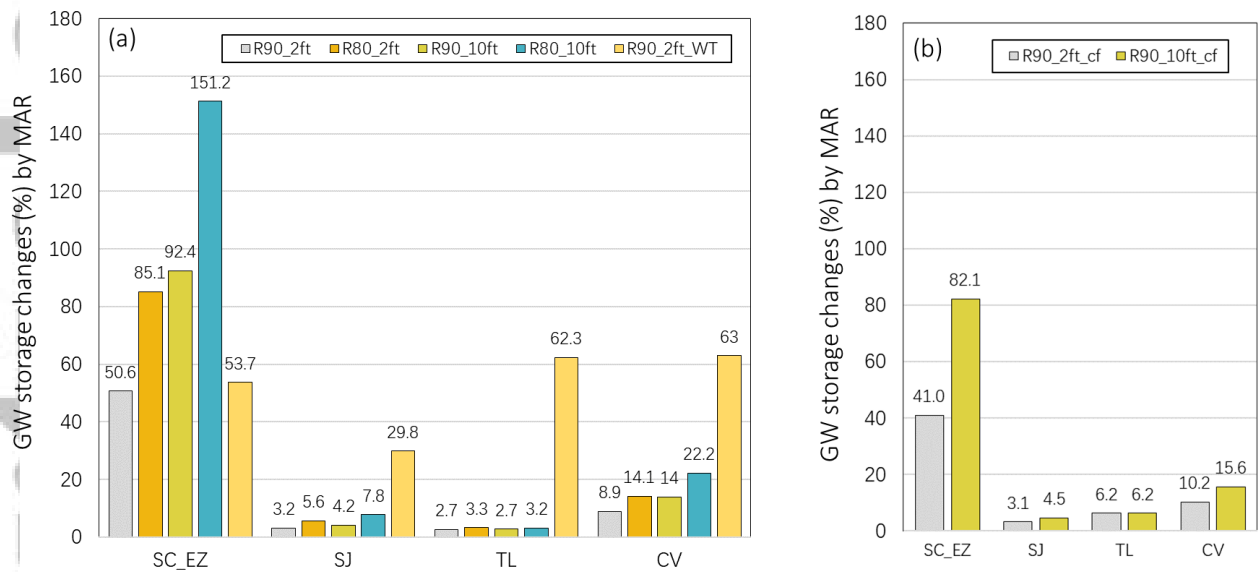
Figure 7. Groundwater storage changes (%) estimated by multiple MAR scenarios, (a) R90_2ft, R80_2ft, R90_10ft, R80_10ft scenarios, and R90_2ft_WT, (b) R90_2ft_cf and R90_10ft_cf scenarios.

4.2.5 Groundwater storage change under current crop/land use scenario

Figure 7b shows the groundwater storage changes due to MAR under current crop/land use and infrastructural development (i.e. R90_2ft_cf and R90_10ft_cf scenarios). We found that the groundwater storage increases for R90_2ft_cf and R90_2ft_cf scenarios are similar to the R90_2ft and R90_2ft scenarios over the entire CV. A regional comparison shows that the groundwater storage increase, compared to the R90_2ft (and R90_10ft) scenario, is lower in SC_EZ, however, it is almost the same in SJ and higher in TL. The results from this experiment indicate that MAR will provide similar benefit (in terms of aquifer storage recovery) in the near future (assuming water supply remains less variable in the next 30–40 years) as it could have done in the past.

4.3 Changes in groundwater balance components

Groundwater storage change in an aquifer is the result of a balance among deep percolation, stream-aquifer interaction, return flow, net subsurface flow, and groundwater pumping. These groundwater balance components are expected to vary among regions. Here, we calculated the cumulative difference in each of the groundwater balance components between MAR and the base scenario using equation (2).

$$\text{Cumulative change } = \frac{\sum_{i=1}^{N} Var_{i,MAR} - \sum_{i=1}^{N} Var_{i,base}}{Total\ years} \qquad (2)$$

where VAR_i represents a particular water balance component for month i. Total years considered are 56 (1960-2015). The units of cumulative change are km^3/year.
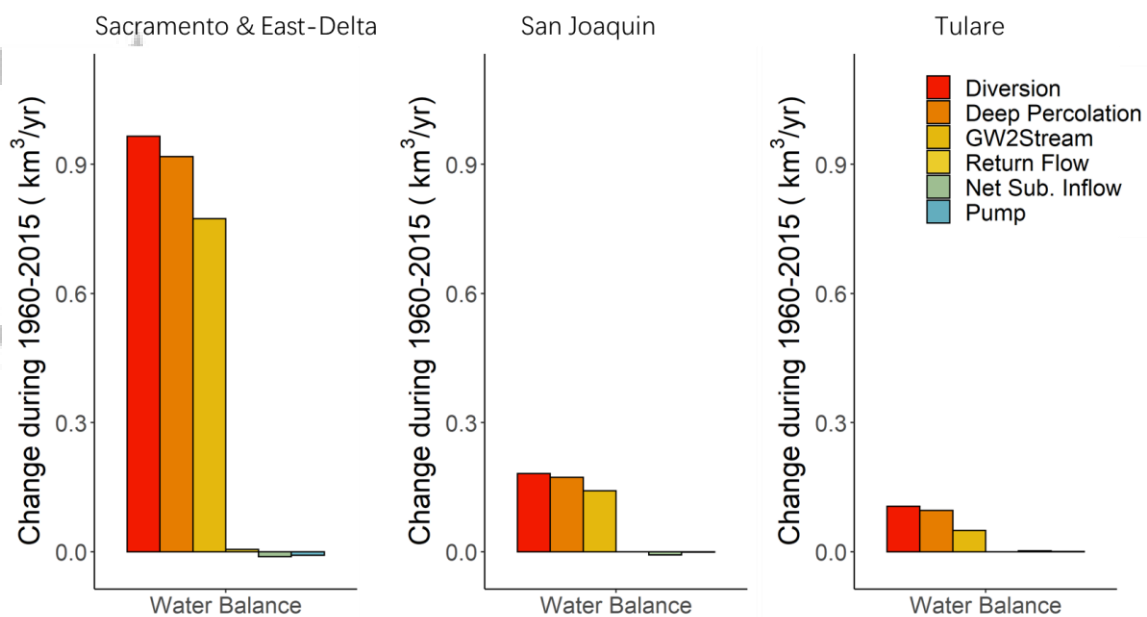
Figure 8. Change in water balance components for R90_2ft scenario compared to base condition averaged over 1960-2015. The water balance components shown here include diversions for MAR, deep percolation, lateral flow from groundwater flow to stream (GW2Stream), net subsurface inflow from neighboring subregions (Net Sub. Inflow), and pumping.

Figure 8 shows the yearly cumulative change in water balance components relative to base conditions in the major regions (i.e., SC_EZ, SJ, and TL) of the CV under the R90_2ft scenario. We show the comparison for R90_2ft only because this scenario's results are representative of the relative contribution of each of the water balance components. In Figure 8, three variables, diversion, deep percolation, and GW flow to stream, show relatively high changes after MAR implementation. Diversion indicates how much water is diverted (from a stream) for MAR. Deep percolation is the portion of diverted water (for MAR) that reaches the saturated zone. Figure 8 shows that the water diversion for MAR is higher in SC_EZ compared to SJ and TL. This is due to higher surface water availability in SC_EZ. As surface water diversions to MAR sites increase, deep percolation also increases in all regions, with a higher rate in SC_EZ and SJ (see Figure S4 of Supplementary Material) than in TL.

The increase in deep percolation also increases lateral flows from groundwater to stream (discussed in the next section). Furthermore, we found that the effect of MAR is not significant on other water balance components, such as return flow, net subsurface inflow, and pumping. The effect of MAR on pumping was low at the regional scale, similar to the finding by Ghasemizade et al. (2019). MAR's influence on groundwater pumping depends on the spatial distribution of MAR sites, head differences between streams and aquifers, hydraulic connectivity, and distances between the MAR sites and streams (Ghasemizade et al., 2019). With MAR, it is possible that streams will not lose as much water to the aquifer due to higher groundwater elevations, which will increase the availability of streamflow for other uses, which in turn could result in a greater decrease in pumping. On the other hand, we found that the regional change in groundwater head after MAR (especially in TL) is modest, therefore the effect on groundwater pumping likely would be small (see Figure S5 for temporal distribution of pumping). We do note that a local level study by Scanlon et al. (2016) on the effect of MAR projects in the southern CV (e.g. Arvin-Edison Water Storage

District, Kern Complex, Rosedale-Rio Bravo and others) shows that groundwater depletion near the MAR projects is much less than the regional depletion. The Scanlon et al. (2016) study also shows that MAR together with conjunctive surface-groundwater use can reduce groundwater pumping rates. We argue that a regional scale decrease in groundwater pumping is only possible when MAR projects can significantly reduce the regionwide depletion ofgroundwater head, which did not occur in our simulated results.

4.4 Changes in stream-aquifer interaction

The net volume of groundwater overdraft recovery is influenced by stream-aquifer interactions (i.e. flow exchange between stream and aquifer). According to Darcy's Law, two factors are important to determine the direction and volume of subsurface flow: (1) horizontal hydraulic conductivity, and (2) head difference between the groundwater table and the connected stream. Higher hydraulic conductivity results in relatively fast movement of subsurface water, and greater positive head differences result in greater movement of water from the aquifer to the stream. In our simulations, all regions had increased flow from the aquifers to the streams (Figure 8) with MAR. To better demonstrate how stream-aquifer interactions vary among regions and over time, we calculated cumulative stream-aquifer interactions using equation (2) for each major CV region.
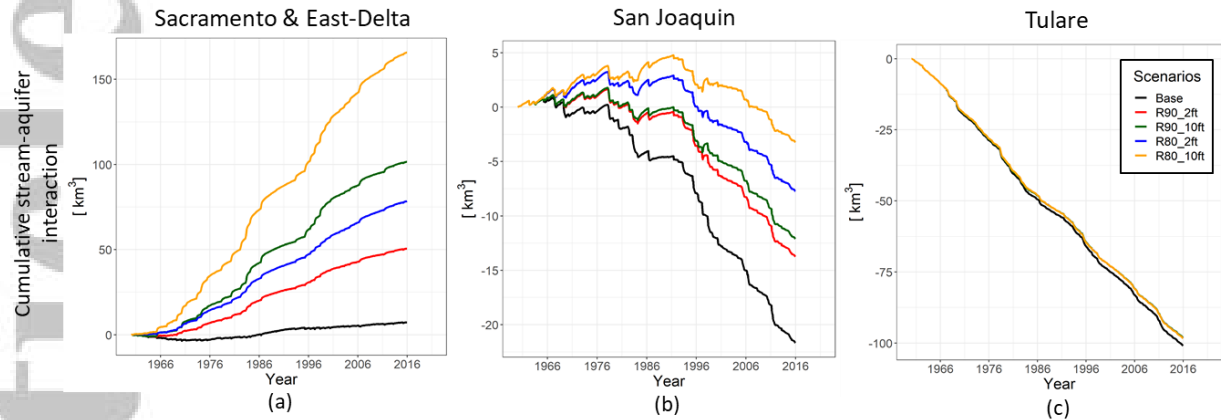
Figure 9. Cumulative stream aquifer interactions in SC_EZ (left), SJ (middle) and TL (right) for the base and MAR scenarios. A positive value indicates flow from groundwater to stream, a negative value indicates vice versa.

Figure 9 shows the cumulative stream-aquifer interactions in SC_EZ, SJ, and TL during 1960-2015. The increase in deep percolation (as shown in Figure 8) associated with MAR raises the groundwater table relative to the base scenario, thereby changing the relative head difference between surface water and the groundwater table. This changes the stream-aquifer dynamics compared to the base scenario. In SC_EZ, the cumulative stream-aquifer interaction is close to 0 for the base condition, but groundwater flow from the aquifer to stream increases under MAR scenarios (Figure 9). This suggests that a fraction of groundwater recharge by MAR returns back to the stream through subsurface flow (or baseflow). In both SJ and TL, cumulative stream-aquifer interactions are negative under the base scenario, which indicates that the groundwater table is lower than the stream stage and there is a net flow from stream to the aquifer in the base condition. As MAR is implemented, the rise in the groundwater table leads to the change in hydraulic head difference and baseflow between the stream and the aquifer. In SJ, the cumulative stream-aquifer exchange is relatively balanced during 1960-1978 under the base condition. However, due to intensive groundwater extraction in SJ in the later part of the simulation period, the groundwater table

dropped substantially and resulted in net negative baseflow even with the implementation of MAR. In TL, the aquifer had been so severely overexploited that it is essentially disconnected from the stream, in which case the recharge rate is theoretically independent of the water table position (Winter et al. 1998; Brunner et al. 2009) and thus insensitive to MAR (as shown in Figure 9c).

4.5 The effect of MAR on low flow augmentation

Summertime (July-September) low flow is an important source of water for fisheries and ecosystem environmental flow. Baseflow (or lateral groundwater flow) from aquifers is an important, often primary, source of summertime low flow. MAR enhances baseflow by increasing net groundwater storage in the aquifers, which can play a vital role in sustaining streamflows during water-scarce drought years. MAR's ability to enhance low flows varies among regions due to variations in soil characteristics (e.g. horizontal and vertical hydraulic conductivity). We analyzed the baseflow change after MAR implementation for our entire simulation period (1960-2015), as well as for 2007-2009 and 2012-2015 drought periods. By comparing the modeled baseflow and the observed summertime streamflow entering the Delta (a proxy of net baseflow during summer), we found the model is in good agreement with observations (see Figure S6 of Supplementary Information).
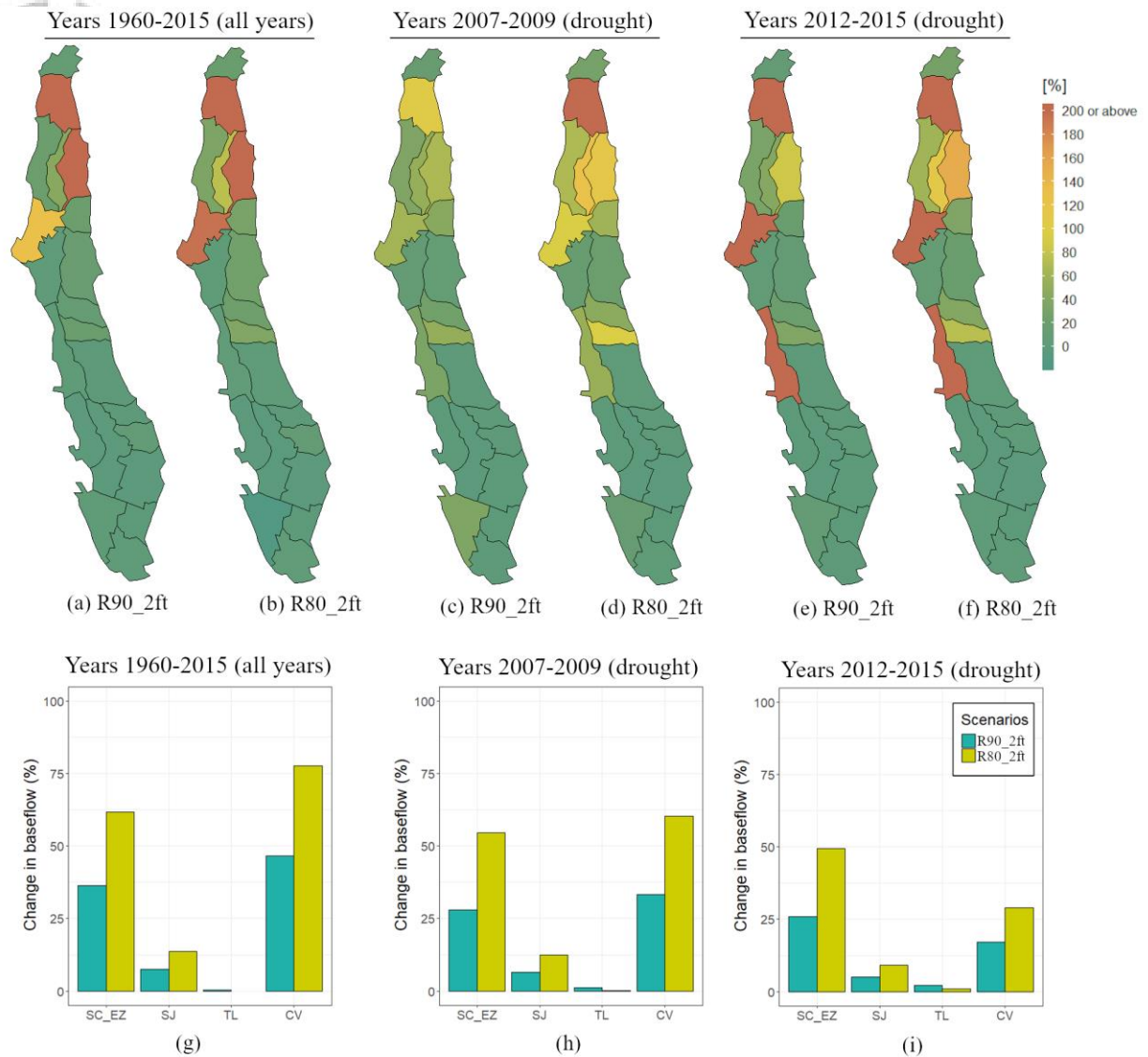
Figure 10. Summertime (July-September) baseflow changes in percentages. (a-f) Spatial distribution of baseflow changes for the entire study period 1960-2015 (a-b), the 2007-2009 drought (c-d) and the 2012-2015 drought (e-f). (g-i) Baseflow changes in major hydrologic regions.

Figures 10 a-f show the spatial distribution of the percent changes in baseflow for the entire simulation period and for the two drought periods. We found that the baseflow increases in almost all subregions in the SC, but is highest in SR-2, SR-5 and SR-6, located around Sacramento River (SR-2 and SR-4) and Feather River (SR-5). In SJ, relatively large increases in baseflow occur in SR-10 and SR-12, near the San Joaquin River (SR-10) and Merced

River (SR-12). In TL, stream-aquifer interactions are weaker, which cause the baseflow to have very low or no change (discussed in Section 4.5).

Figures 10g-i show bar charts of the percent changes in baseflow. The figures show that there is a net increase in baseflow of about 47% and 78% under the R90_2ft and R80_2ft scenarios, respectively, during 1960-2015 in CV (Figure 10g). The northern region (SC_EZ) generally has the greatest increases in baseflow due to higher MAR-induced groundwater storage. Baseflows increase by about 37% and 62% in SC_EZ and 7% and 13% in SJ under the R90_2ft and R80_2ft scenarios, respectively, during 1960-2015 (Figure 10g). In TL, the baseflow increases are relatively small (~1%). Therefore, MAR appears to be a promising way to ensure environmental and ecological flows. In addition, we also computed the baseflow changes under R90_10ft and R80_10ft scenarios during 1960-2015 (not shown in Figure 10), which are about 85% and 146% in SC_EZ and 9% and 18% in SJ respectively. As a comparison, Ghasemizade et al. (2019) found the ratio of baseflow increase and MAR water delivery volume to be 0.38-0.49 in SR-18 (for the period of 1921 to 2009), whereas we found the ratio to be 0.30-0.39 for the same subregion.

MAR is intended to promote drought resilience through groundwater banking in the wet years (Scanlon et al. 2016). To evaluate the extent to which this would be the case, we compared baseflow changes during the 2007-2009 and 2012-2015 droughts. Figures 10h-i show the percent changes in baseflow during the 2007-2009 and 2012-2015 droughts, respectively. The baseflow increase due to MAR is substantial in most of the subregions during the drought years. We found that MAR would increase baseflow over the entire CV by around 28% (R90_2ft) and 60% (R80_2ft) during the 2007-2009 drought, and around 17% (R90_2ft) and 29% (R80_2ft) during the 2012-2015 drought. SC has the highest enhanced baseflow among all regions. As the baseflow increase was found to be positively related to

the amount of water applied for MAR, almost all of the subregions show higher increases under the R80_2ft than R90_2ft scenario. However, baseflow increases in SR-15 and SR-19 are lower under the R80_2ft than the R90_2ft scenario. This is because MAR diversion nodes for both subregions are located downstream of other diversion nodes that deliver MAR to other subregions first. Kings River delivers MAR water to SR-17 first and then SR-15, whereas Kern River delivers MAR water to SR-21 first and then SR-19. In SR-15 and SR-19, the actual volumes of water applied for MAR are 0.01 and 1.36 km^3 lower in the R80_2ft scenario than in the R90_2ft scenario. Overall, MAR can augment summertime low flows, especially during drought periods, by as much as 52% without water transfer and 73% if excess flows are delivered from north to south. This finding confirms that MAR could enhance drought resilience and sustain environmental flows in the CV.
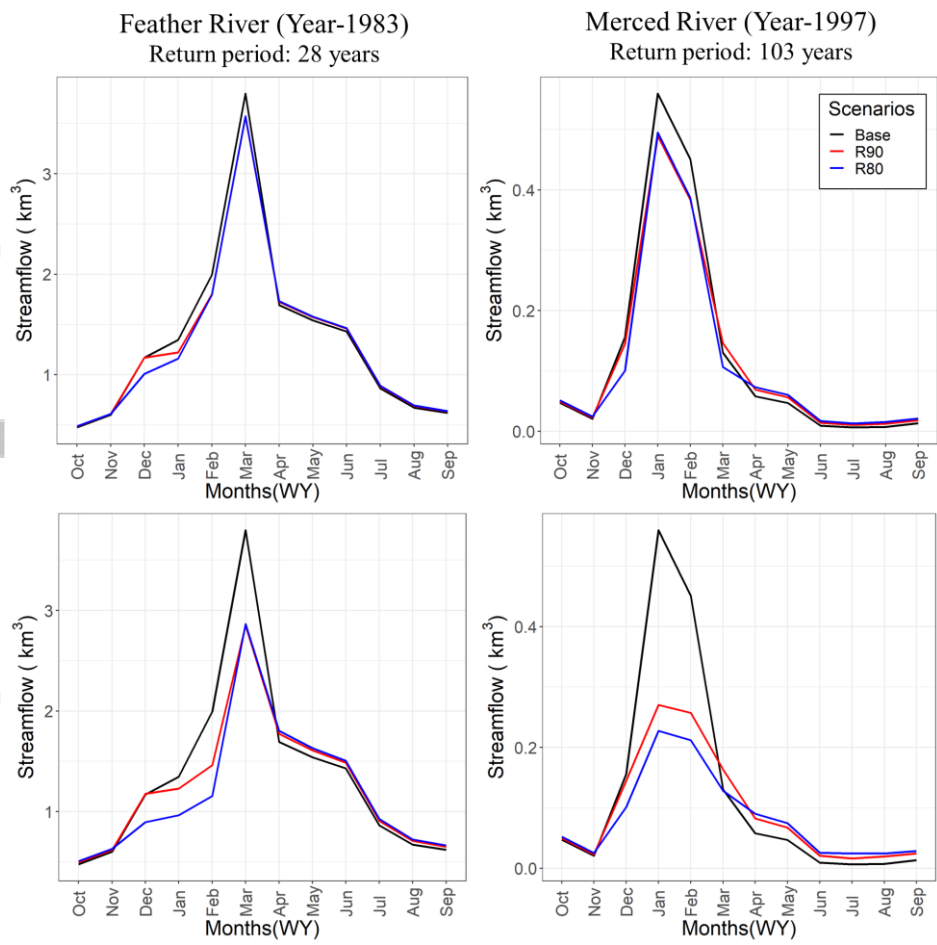
Figure 11. Monthly hydrograph for two wet years (1983 and 1997) near the outlets of Feather River (top row) and Merced River (bottom row). In all the plots, the black line represents the base simulation, and the red and blue lines in the top row represent R90_2ft and R80_2ft scenarios respectively and in the bottom row represent R90_10ft and R80_10ft scenarios respectively.

4.6 The effect of MAR on flood risk reduction

MAR could reduce flood peaks by diverting high flows from the streams. Figure 11 shows the monthly hydrograph of the Feather River in 1983 and the Merced River in 1997 – two major flood events in the CV. The peak discharge in both basins usually occurs between January and March. We found that the peak discharge decreases in all cases with the MAR implementation. The comparison of the scenarios with different maximum depths (2ft and 10ft) show that much greater reduction in flood peak occurs (Figure 11) when the maximum allowable depth is increased from 2ft to 10ft, especially during the extreme Merced River flood of 1997 (an estimated return period of 103 years). Overall, we found peak flow decreased by around 10%-40% (during February-March) in Feather River and 12%-59% (during January-February) in Merced River.

4.7 Potential crop damage due to waterlogging

MAR implementation raises the water table, which can threaten crops if the water table enters the root zone. Root zone waterlogging can have multiple negative consequences, such as reduced aeration, slowed bacterial activity, and increased plant vulnerability to diseases. We identified locations that are at risk of crop damage due to root zone waterlogging. The average root zone depth for both row and tree crops is 1.5 m in the model, which was also used by Ghasemizade et al. (2019). As a metric of risk, we calculated the number of additional months when the water table was below the threshold depth under MAR scenarios

during the growing season (Figure 12) and the winter seasons (Figure S7 of the Supplementary Information). All the subregions in SC have some (non-zero) risk associated with rootzone water logging. In SJ, areas in subregions 11-13 shows increased waterlogging, but the waterlogging is not expected to last more than about 20% of the growing season months. In TL, there are a few areas in subregions 18 and 19 that show increased waterlogging (mostly <40% of the time waterlogged) under R90_2ft_WT scenario. Despite the waterlogging expected to occur in some areas under R90_2ft_WT scenario, most places in the domain encounter waterlogging during less than 5% of the growing season. This analysis indicates that more detailed investigation of the waterlogging problem will be warranted in the future work. Although the rules we use to determine where excess flows are to be applied do not consider waterlogging, the model and the scenario settings could be further refined to reduce the extent and magnitude of waterlogging risk.
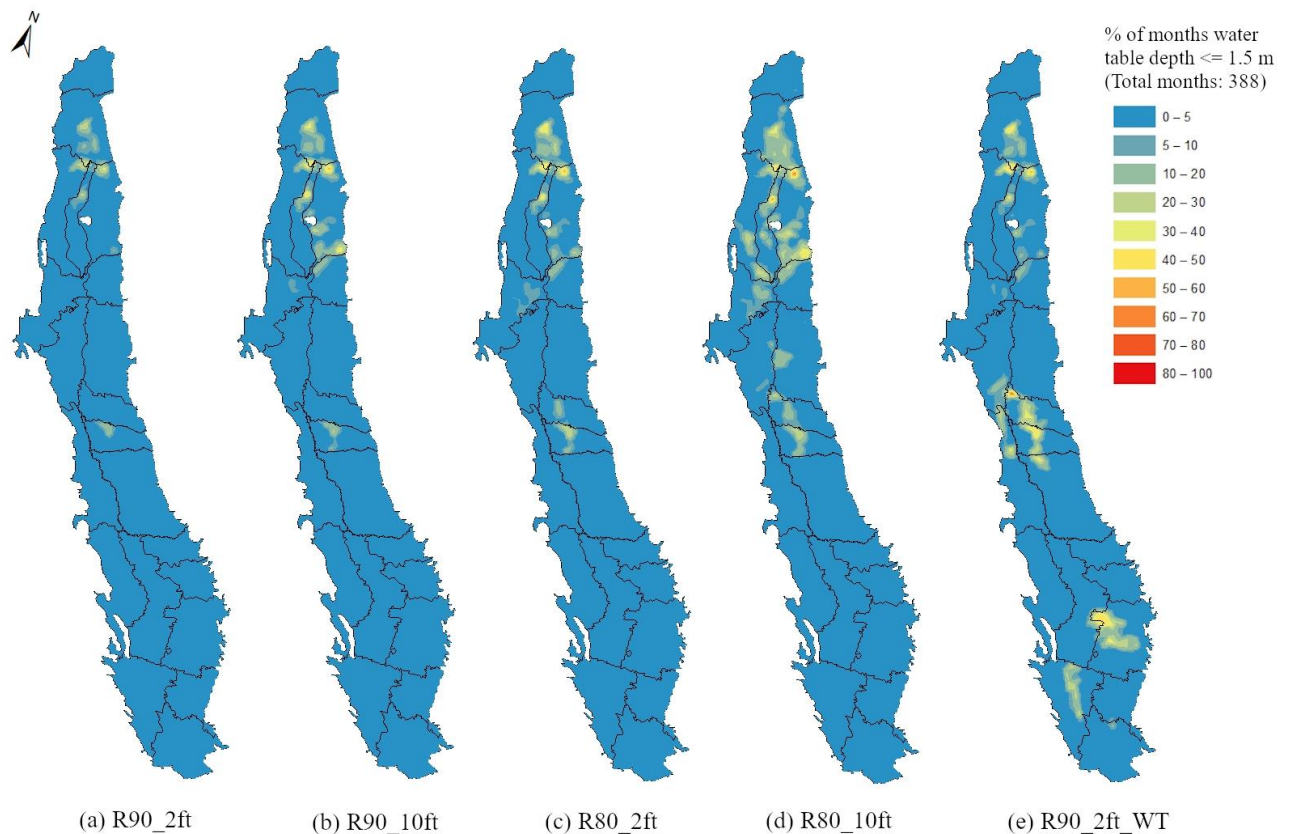

(a) R90_2ft   (b) R90_10ft   (c) R80_2ft   (d) R80_10ft   (e) R90_2ft_WT

Figure 12. Percent of growing season months (April through October) for which the water table enters the rootzone due to the implementation of different MAR scenarios.

4.8 Limitations and future research

Our results are based on several important assumptions, which infer certain limitations to our findings. First, we assume that there are adequate water delivery facilities to convey surface water to the MAR recharge sites when flood water is available for recharge. Clearly, this may not always be the case, and in this respect our results are indicative of the maximum potential of MAR. Second, we used a monthly time step for the model (a C2VSIM limitation), which limits our ability to capture peak streamflows that arise from short-term storm events. While our results show that there could be considerable flood protection benefits from the use of MAR, further studies (at shorter time steps) are needed to reliably quantify those benefits. Third, in our computations, we assume that the areas selected for MAR would be available for recharge regardless of policy and social constraints that may limit the use of that land (Foster and Garduño, 2013; Li et al., 2016; Deitch and Dolman, 2017). These constraints include, but are not limited to, legal/regulatory frameworks, groundwater governance structure, local water policies, landowners' participation willingness, existing water rights, and coordination among agencies (see CDWR 2018b for more detail). As is the case for our assumption of adequate conveyance infrastructure, these considerations suggest that our results are best interpreted as an upper bound on the potential of MAR to mitigate groundwater overdrafts. Fourth, we note that the depth of water to be applied was not differentiated among different SAGBI classes. The differences in recharge rates among specific recharge sites might result in variable benefits of MAR. A more detailed investigation is needed to determine the effects of such differences on the field-scale potential for MAR. Lastly, we did not link the role of MAR to climate change. However, this was

partially addressed in a previous study (Alam et al., 2019). An expected increase in the winter inflows to the CV may be expected to provide more water for MAR in the future.

5. Summary and Conclusions

Groundwater plays a vital role in the Central Valley's water supply, especially during drought periods. Over our 56-year study period (1960-2015), groundwater storage in the CV has progressively decreased by an average of around 3 km^3/year. MAR has the potential to replenish groundwater through the application of high winter flows to agricultural lands. Our objective was to evaluate the potential of groundwater overdraft recovery and other ancillary benefits through a regionwide implementation of MAR. We conducted numerical experiments using a surface water-groundwater hydrological model and assuming wintertime flows exceeding the 90th (R90 scenarios) and 80th (R80 scenarios) percentiles were available to be applied for MAR. Based on our simulations, we conclude that:

- MAR could potentially recover 9 – 22% (for R90 and R80 scenarios) of the existing groundwater overdraft aggregated over the entire CV. The effect of MAR varies among regions. In the northern CV (i.e. Sacramento) where groundwater depletion is not a major problem (compared to the southern CV), the effect of MAR is high. In southern CV (i.e. San Joaquin and Tulare) where groundwater overdraft is large, MAR cannot solve the problem. We find that the contribution of MAR to the reduction of the historic groundwater overdraft would be about 3 – 8% in the San Joaquin (SJ) region, and even less (about 3%) in the Tulare (TL) region. The primary cause of low groundwater recovery in the southern CV (SJ and TL regions) is the lack of adequate headwater supply in relation to the large existing groundwater overdraft.

- The application of MAR using streamflow crossing each region is not expected to effectively mitigate the groundwater overdraft problem in the southern CV. However, MAR could mitigate a much greater portion of the groundwater overdraft through the delivery of excess winter flow from northern CV to southern CV for MAR. We investigated the effect of delivering excess winter Delta outflow (over the 90th percentile) to the southern CV for MAR, this would enhance groundwater overdraft recovery by 63% in CV, 30% in SJ, and 62% in TL.

- The application of MAR would have ancillary benefits in addition to groundwater overdraft recovery. MAR can augment summertime low flows, especially during drought periods by as much as 52% without water transfer and 73% if excess flows are delivered from north to south. Moreover, we tested the effect of MAR on streamflow of Feather River and Merced River during two large flood events, showing that MAR effectively reduces the flood peaks by 10% – 40% in Feather River and 12% – 59% in Merced River.

References

Alam, S., Gebremichael, M., Li, R., Dozier, J., and Lettenmaier, D. P. (2019). Climate change impacts on groundwater storage in the Central Valley, California. Climatic Change, 157(3-4), 387-406.

Alley, W. M., Healy, R. W., LaBaugh, J. W., and Reilly, T. E. (2002). Flow and storage in groundwater systems. Science, 296(5575), 1985–1990.

Bachand, P. A. M., Roy, S. B., Choperena, J., Cameron, D., and Horwath, W. R. (2014). Implications of using on-farm flood flow capture to recharge groundwater and mitigate flood risks along the Kings River, CA. Environmental Science and Technology, 48(23), 13,601–13,609. https://doi.org/10.1021/es501115c

Baker D B, Richards R P, Loftus T T and Kramer J W 2004 A new flashiness index: characteristics and applications to midwestern rivers and streams J. Am. Water Resour. As. 40 503–22

Brown, L. R., Kimmerer, W., and Brown, R. (2009). Managing water to protect fish: a review of California's environmental water account, 2001–2005. Environmental management, 43(2), 357-368.

Brush, C.F., Dogrul, E.C. and Kadir, T.N., 2013. *Development and calibration of the California Central Valley Groundwater-Surface Water Simulation Model (C2VSim), version 3.02-CG*. Bay-Delta Office, California Department of Water Resources.

Brunner, P., P.G. Cook, and C.T. Simmons. 2009. Hydrogeologic controls on disconnection between surface water and groundwater. Water Resources Research 45, W01422. DOI:10.1029/2008WR006953.

Brush, C.F. 2013. Historical Rim Inflows, Surface Water Diversions and Bypass Flows for C2VSIM. Bay-Delta Office, California Department of Water Resources.

California Law (2014). *Sustainable Groundwater Management*. Retrieved from http://leginfo.legislature.ca.gov/faces/codes_displayexpandedbranch.xhtml?tocCode=WAT&division=6.&title=&part=2.74.&chapter=&article

California Department of Water Resources and California Natural Resources Agency, and State of California (2013). California's Groundwater Update 2013, A Compilation of Enhanced Content for California (California: Department of Water Resources) pp 1–90

California Department of Water Resources (2019). Flood-MAR research and data development plan. The Flood-MAR Research Advisory Committee, Sacramento, CA, USA.

California Department of Water Resources (2018a). Water Available for Replenishment. Appendix A: Water Available for Replenishment Information and Estimates

California Department of Water Resources (2018b). Flood-MAR white paper: using flood water for managed aquifer recharge to support sustainable water resources. Sacramento, CA, USA.

Christian-Smith, J., Levy, M.C. and Gleick, P.H., 2015. Maladaptation to drought: a case report from California, USA. Sustainability Science, 10(3), pp.491-501.

Christian-Smith, J., 2013. Improving Water Management through Groundwater Banking: Kern County and the Rosedale-Rio Bravo Water Storage District.

Chinnasamy, P., Muthuwatta, L., Eriyagama, N., Pavelic, P. and Lagudu, S., 2018. Modeling the potential for floodwater recharge to offset groundwater depletion: a case study from the Ramganga basin, India. Sustainable Water Resources Management, 4(2), pp.331-344.

Dahlke, H. E., Brown, A. G., Orloff, S., Putnam, S., and O'Geen, A. (2018). Managed winter flooding of alfalfa recharges groundwater with minimal crop damage. California Agriculture, 72(1), 1–11. https://doi.org/10.3733/ca.2018a0001

Deitch, M. J., and Dolman, B. (2017). Restoring summer baseflow under a decentralized water management regime: Constraints, opportu- nities, and outcomes in Mediterranean-climate California. Water, 9(1), 29. https://doi.org/10.3390/w9010029

Dillon, P., Stuyfzand, P., Grischek, T., Lluria, M., Pyne, R.D.G., Jain, R.C., Bear, J., Schwarz, J., Wang, W., Fernandez, E. and Stefan, C., 2019. Sixty years of global progress in managed aquifer recharge. Hydrogeology journal, 27(1), pp.1-30.

Dillon, P.J., Pavelic, P., Page, D., Beringen, H. and Ward, J., 2009. Managed aquifer recharge. An introduction waterlines report series, 13.

Dogrul, E.C., Kadir, T.N., Brush, C.F. and Chung, F.I., 2016. Linking groundwater simulation and reservoir system analysis models: The case for California's Central Valley. Environmental modelling and software, 77, pp.168-182.

Dogrul, E. C., Kadir, T. N., and Brush, C. F. (2017). DWR Technical Memorandum: Theoretical Documentation and User's Manual for IWFM Demand Calculator (IDC-2015), Revision 63, August 2017, Sacramento, 312 pages.

Famiglietti, J. S., Lo, M., Ho, S. L., Bethune, J., Anderson, K. J., Syed, T. H., et al. (2011). Satellites measure recent rates of groundwater depletion in California's Central Valley. Geophysical Research Letters, 38, L03403. https://doi.org/10.1029/2010GL046442

Faunt, C.C., Belitz, K., Hanson, R.T., 2009. Groundwater Availability of the Central Valley Aquifer, California. Chapter B: Groundwater Availability in California's Central Valley., Groundwater Resources Program.

Flores-López, F. (2019). Managed Aquifer Recharge Using Floodwaters on Agricultural Fields. California Department of Water Resources. https://www.grac.org/media/files/files/c42cafa7/19-4-1-c-francisco-flores-lopez.pdf

Fogg, G. E. (1986). Groundwater flow and sand body interconnectedness in a thick, multiple-aquifer system. Water Resources Research, 22(5), 679-694.

Foster, S. and Garduño, H. (2013). Groundwater-resource governance: are governments and stakeholders responding to the challenge?. Hydrogeology Journal, 21(2), pp.317-320.

Ghasemizade, M., Asante, K.O., Petersen, C., Kocis, T., Dahlke, H.E. and Harter, T., 2019. An integrated approach toward sustainability via groundwater banking in the southern Central Valley, California. Water Resources Research, 55(4), pp.2742-2759.

Gorelick, S. M., and Zheng, C. M. (2015). Global change and the groundwater management challenge. Water Resources Research, 51, 3031–3051. https://doi.org/10.1002/2014WR016825

Hanak, E., Escriva-Bou, A., Gray, B., Green, S., Harter, T., Jezdimirovic, J., Lund, J., Medellín-Azuara, J., Moyle, P. and Seavy, N. (2019). Water and the Future of the San Joaquin Valley. Public Policy Institute of California.

Hanak, E., Jezdimirovic, J., Green, S., and Escriva-Bou, A. (2018). Replenishing Groundwater in the San Joaquin Valley. Public Policy Institute of California, 36.

Hanak, Ellen, Jay Lund, Brad Arnold, Alvar Escriva-Bou, Brian Gray, Sarge Green, Thomas Harter, Richard Howitt, Duncan MacEwan, Josué Medellín-Azuara, Peter Moyle, Nathaniel Seavy. 2017. Water Stress and a Changing San Joaquin Valley. Public Policy Institute of California.

Hanson, R. T., Flint, L. E., Flint, A. L., Dettinger, M. D., Faunt, C. C., Cayan, D., and Schmid, W. (2012). A method for physically based model analysis of conjunctive use in response to potential climate changes. Water Resources Research, 48(6).

Hashemi, H., Berndtsson, R., and Persson, M. (2015). Artificial recharge by floodwater spreading estimated by water balances and groundwater modelling in arid Iran. Hydrological Sciences Journal, 60(2), 336-350.

Kocis, Tiffany N., and Helen E. Dahlke. "Availability of high-magnitude streamflow for groundwater banking in the Central Valley, California." *Environmental Research Letters* 12, no. 8 (2017): 084009.

Kourakos, G., Dahlke, H.E. and Harter, T., 2019. Increasing Groundwater Availability and Seasonal Baseflow through Agricultural Managed Aquifer Recharge in an Irrigated Basin. Water Resources Research.

Li, R., Ou, G., Pun, M., and Larson, L. (2018). Evaluation of Groundwater Resources in Response to Agricultural Management Scenarios in the Central Valley, California. Journal of Water Resources Planning and Management, 144(12), 04018078.

Li, R., Pun, M., Bradley, J., Ou, G., Schneider, J., Flyr, B., Winter, J. and Chinta, S. (2016). Evaluating hydrologically connected surface water and groundwater using a groundwater model. JAWRA Journal of the American Water Resources Association, 52(3), pp.799-805.

Maples, S. R., Fogg, G. E., and Maxwell, R. M. (2019). Modeling managed aquifer recharge processes in a highly heterogeneous, semi-confined aquifer system. Hydrogeology Journal, 27(8), 2869-2888.

Niswonger, R.G., Morway, E.D., Triana, E. and Huntington, J.L., 2017. Managed aquifer recharge through off-season irrigation in agricultural regions. Water Resources Research, 53(8), pp.6970-6992.

O'Geen, A., Saal, M., Dahlke, H., Doll, D., Elkins, R., Fulton, A., et al. (2015). Soil suitability index identifies potential areas for groundwater banking on agricultural lands. California Agriculture, 69,75–84. https://doi.org/10.3733/ca.v069n02p75

Olden J D and Poff N L 2003 Redundancy and the choice of hydrologic indices for characterizing streamflow regimes River Res. Appl. 19 101–121

Perrone D and Merri Rohde M 2016 Benefits and economic costs of managed aquifer recharge in California San Francisco Estuary and Watershed Science 14 1–13

Roddell, M., I. Velicogna, and J.S. Famiglietti 2009. Satellite-based estimates of groundwater depletion in India. Nature, 460 999-1002, doi: 10.1038/nature08238.

Ronayne, M. J., Roudebush, J. A., and Stednick, J. D. (2017). Analysis of managed aquifer recharge for retiming streamflow in an alluvial river. Journal of hydrology, 544, 373-382.

Scanlon, B. R., Faunt, C., Longuevergne, L., Reedy, R., Alley, W. M., McGuire, V. L., and McMahon, P. B. (2012). Groundwater depletion and sustainability of irrigation in the US High Plains and Central Valley. Proceedings of the National Academy of Sciences

Scanlon, B. R., Reedy, R. C., Faunt, C. C., Pool, D., and Uhlman, K. (2016). Enhancing drought resilience with conjunctive use and managed aquifer recharge in California and Arizona. Environmental Research Letters, 11(3), 035013.

Siebert, S., Burke, J., Faures, J. M., Frenken, K., Hoogeveen, J., Doll, P., and Portmann, F. T. (2010). Groundwater use for irrigation—A global inventory. Hydrology and Earth System Sciences, 14(10), 1863–1880. https://doi.org/10.5194/hess-14-1863-2010

Sprenger, C., Hartog, N., Hernández, M., Vilanova, E., Grützmacher, G., Scheibler, F., and Hannappel, S. (2017). Inventory of managed aquifer recharge sites in Europe: Historical development, current situation and perspectives. Hydrogeology Journal, 25(6), 1909–1922. https://doi.org/10.1007/s10040-017-1554-8

Taylor, R.G., Scanlon, B., Döll, P., Rodell, M., Van Beek, R., Wada, Y., Longuevergne, L., Leblanc, M., Famiglietti, J.S., Edmunds, M. and Konikow, L., 2013. Ground water and climate change. Nature climate change, 3(4), pp.322-329.

USGS (United States Geological Survey) 2016 Daily Streamflow Conditions, USGS Current Water Data for the Nation http://waterdata.usgs.gov/nwis/rt

Wada, Y., van Beek, L. P., van Kempen, C. M., Reckman, J. W., Vasak, S., and Bierkens, M. F. (2010). Global depletion of groundwater resources. Geophysical Research Letters, 37, L20402.

Winter, T.C., J.W. Harvey, O.L. Franke, and W.M. Alley, 1998. Ground Water and Surface Water: A Single Resource. U.S. Geological Survey Circular 1139. http://pubs.water.usgs.gov/cir1139

Xiao, M., Koppa, A., Mekonnen, Z., Pagán, B. R., Zhan, S., Cao, Q., Aierken, A., Lee, H. and Lettenmaier, D. P. (2017). How much groundwater did California's Central Valley lose during the 2012–2016 drought?. Geophysical Research Letters, 44(10), 4872-4879.